Self-collimation in an atomic beam evaporated from a superfluid ^{4}He film

H. H. Hjort and D. O. Edwards
Physics Department, The Ohio State University, 174 West 18 Avenue, Columbus, Ohio 43210
(Received 19 November 1999)

Using a scaling Monte Carlo method, we have simulated the scattering in a pulsed atomic beam evaporated from a superfluid ^{4}He film. The simulation assumes that the atoms leaving the surface have the equilibrium Maxwellian distribution at the temperature of the film T. This means that the initial particle flux varies as cos θ (Lambert's law). We find that the effect of atomic scattering just above the film is to bias the flux in favor of the forward (small θ) direction, in agreement with the experiment of Eckardt *et al.* The simulation predicts that the deviation from Lambert's law grows rapidly with increasing heat input Q and decreasing pulse length. At the same time, the average kinetic energy per particle in the forward direction is enhanced relative to the global average, $2k_BT$. The distribution with respect to speed is narrower than Maxwellian in the forward direction but broader at large angles. We find that a beam that has passed through a slit is slightly narrower than in a ballistic calculation with no collisions. This effect seems to saturate at values of Q that correspond to 30 or 40 collisions per atom.

PACS number(s): 34.50.−s, 39.10.+j, 02.70.Lq

I. INTRODUCTION

A convenient way to produce a low energy ^{4}He atomic beam is by the pulsed evaporation of the superfluid film. Such beams have been used to study the angular and speed distributions of evaporated atoms [1–3], to measure the reflection coefficient of atoms at the surface of liquid ^{4}He [4–6], and to measure the atomic scattering cross section [7,8]. With small heat pulses, the atoms are usually assumed to propagate ballistically, with negligible intrabeam scattering. With large heat inputs, the intrabeam scattering makes the distribution of speeds more homogeneous [9]. This corresponds to cooling in the center of the mass frame [10].

The experiments of Eckardt *et al.* [1] showed that, for a very small heat input, the angular distribution deviated from Lambert's law although the distribution in speed was close to Maxwellian [1,2]. One explanation is that the thermal excitations in the film producing the evaporated atoms do not have an equilibrium distribution. Another, suggested by Meyer [11], is that the deviations from Lambert's law are caused by atomic scattering near the surface of the film.

In this paper we simulate the experiments of Eckardt *et al.* to discover the origin of the angular distribution and to explore the consequences for other experiments using the same technique. In the simulation we assume that, when the atoms leave the film, their distribution is Maxwellian and obeys Lambert's law. We find that the atomic scattering near the film produces the distribution seen at large distances, as suggested by Meyer.

II. METHOD

We have recently simulated [12] a low temperature experiment using two pulsed low-intensity atomic beams. This was proposed to measure the ^{4}He-^{4}He scattering cross section $\sigma(v_r)$ for small relative speed v_r. Calculated values of σ are shown in Fig. 1. Because of the existence [13] of a weakly bound dimer (~ 1 mK), $\sigma(0)$ is expected [14] to be unusually large, about 1.83×10^5 Å^2. We showed that σ can be accurately measured in the appropriate range of v_r so as to determine $\sigma(0)$. The simulation assumed the velocity distribution at 40 mm from the film to be the one experimentally observed by Eckardt *et al.* [1].

In this paper, we use the same scaling Monte Carlo method [12,15] to study the origin of this distribution by following the trajectory of each particle from the moment it leaves the surface of the film. The calculation includes multiple scattering but excludes three-body collisions. Details of the method are described in Ref. [12]. Here we give a brief summary.

The number of atoms N evaporated by a typical small heat pulse, 10 nJ, is about 10^{14}. To make the computation of the trajectories manageable, we reduce the number of particles $n=N/\lambda$ in the simulation by a large scaling factor λ, while increasing the cross-section $\sigma(v_r)$ by λ. As shown in Refs. [12,15] the scattering rate per particle remains unchanged. Following Ref. [12], we refer to atoms in the unscaled system and particles in the scaled system.

In low temperature experiments, only s-wave scattering contributes significantly to the collisions. We calculate the

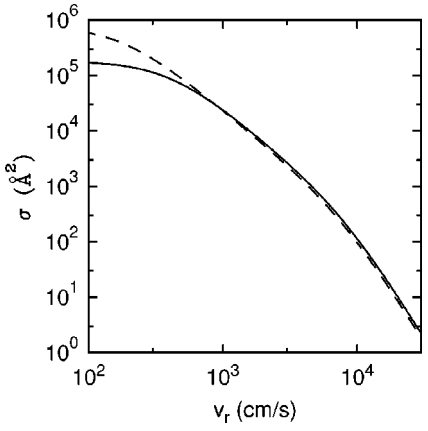

FIG. 1. Plot of the cross section $\sigma(v_r)$ vs relative velocity v_r for the SAPT2 potential (full curve) and for the Lennard–Jones potential (dashed curve).

s-wave cross section using effective range theory [16,17] with parameters, the most accurate available, calculated from the SAPT2 potential [14,18]

$$\sigma = \frac{8\pi a_0^2}{\left(1-\frac{1}{2}a_0 r_0 k^2\right)^2 + (a_0 k)^2}. \tag{2.1}$$

Here $a_0 = 85.25$ Å is the scattering length and $r_0 = 7.256$ Å is the effective range. The relative wave vector is $k = m_4 v_r/2\hbar$ where m_4 is the atomic mass.

Figure 1 is a plot of $\sigma(v_r)$ versus the relative speed v_r. For comparison we also show σ from the parameters for the classic Lennard–Jones potential, $a_0 = -176.3$ Å and $r_0 = 7.957$ Å [11]. With the Lennard–Jones potential, the dimer is not quite bound. At speeds above 3×10^3 cm/s it gives a cross section about 15% smaller than the SAPT2, although $\sigma(0)$ is over four times larger.

From the scaled cross-section $\lambda\sigma(v_r)$ we get the particle collision distance $r_c(v_r) = \sqrt{\lambda\sigma(v_r)/\pi}$. To collide, two particles must have a distance of closest approach less than $r_c(v_r)$. Since the scattering is *s* wave, the trajectories of the colliding particles are modified by giving their relative velocity v_r a new random orientation. The new trajectories start from the positions of closest approach [12].

The scaling method breaks down when the largest collision distance $r_c(0) = \sqrt{\lambda\sigma(0)/\pi}$ approaches the size of other lengths in the system. The smallest length in our simulation is the size of the heater, 8 mm by 8 mm. This sets an upper limit on λ. On the other hand, the computation time for a simulation is proportional to N^3/λ^2. [The number of collisions is proportional to $\lambda n(n-1)$. After each collision we must recalculate the collisions that might occur with the $n-2$ other particles. Thus, the time is proportional to $\lambda n(n-1)(n-2) \sim N^3/\lambda^2$.]

Each simulation may be repeated S times to improve the statistical accuracy, proportional to $1/\sqrt{nS}$. Therefore, for a given accuracy, the total computation time increases as N^2/λ. Unlike our previous program [12], this one was written in FORTRAN. It is available on an Internet web site [19].

We ran the program for various nominal heat inputs Q_0 and pulse lengths 2τ centered at $t=0$. The particles evaporated during the pulse leave the surface of the film with a Maxwellian distribution at temperature T. We determined T by equating the energy of the evaporated atoms to Q_0. Some of the atoms are almost immediately scattered back into the film. Their energy was subtracted from Q_0 to give Q, the heat carried away from the film. The difference between Q_0 and Q depends on the intensity of the pulse. For our largest heat input $Q_0 = 56.5$ nJ, the value of Q is 47 nJ. For our simulation of the angular distribution experiment in Ref. [1], the difference between $Q_0 = 2.9$ nJ and $Q = 2.7$ nJ is quite small.

In an actual experiment, some of the heat is conducted away and some is needed to raise the temperature of the film and heater. Also, the evaporation rate varies during the heat pulse and it continues for a short time afterwards. These complications make a strict quantitative comparison with experiments quite difficult. A calculation of some of these effects is given in Ref. [20].

Most of the simulations were run in two configurations. In the first, we calculated the energy flux into a hemispherical dome 35 mm distant from the center of the heater. This was the distance between the heater and the detector in the angular distribution experiment in Eckardt *et al.* The dome was divided into 100 zones evenly spaced in $\cos\theta$ so that each covered the same solid angle. Here θ is measured with respect to the normal to the heater.

In the second configuration we placed the heater at a distance of 41 mm from a 10×16 mm^2 window in a planar screen. An 8×8 mm^2 detector was moved on an arc of radius 41 mm from the center of the window. This geometry reproduces that in the beam experiments of Refs. [1,3]. To define the volume of the simulation the apparatus was surrounded by a sphere of radius 45 mm.

Whenever a particle hits a surface, it is assumed to be absorbed, in agreement with experiments [4–6] that show the reflection coefficient to be small except at glancing incidence. The energy deposited includes the latent heat [21] $L_4/k_B = 7.17$ K as well as the kinetic energy.

Our method includes only binary collisions; it does not consider three body collisions. We make an estimate of the ratio of three body to two body collisions by considering a small spherical volume of radius $\sqrt{\bar{\sigma}/\pi}$, centered on a particular atom. Here $\bar{\sigma}$ is the mean unscaled cross section observed in our simulations, about $0.05\sigma(0)$. We compare the probabilities that one or two other atoms are within the sphere. These probabilities are largest next to the film during the pulse.

At the surface of the film, the density is $\sim P/2k_BT$ where $P(T)$ is the vapor pressure. We include the factor of two because atoms are mainly moving away from the film. Our highest heat input ($Q = 47$ nJ), with $2\tau = 30$ μs, corresponds to $T = 0.67$ K. The ^{4}He vapor pressure [22] at this temperature is 1.6 dyn/cm^2, giving a density of 8.5×10^{15} atoms per cm^3. From this density and the Poisson distribution, the probability of finding two or more atoms within the sphere is 0.3% of that for finding one atom. If we use the maximum possible cross-section $\sigma(0)$, instead of $\bar{\sigma}$, the ratio increases to 30%. Since this is the worst case, we assume the effect of three body scattering to be small.

Without three body collisions, no dimers can form in our beam. However, this is not important until the temperature in the center of mass approaches the binding energy, about 1 mK. We are very far from this regime in all the simulations described here.

III. RESULTS

A. Number of collisions

Although three-body collisions are neglected, multiple collisions are important. This is illustrated in Fig. 2 which shows, for the average evaporated atom, the number of collisions per mm as a function of the distance from the film. The dashed and dotted curves, for $Q_0 = 2.9$ nJ, $2\tau = 30$ and 60 μs, were calculated analytically assuming that the distribution at all z is the original Maxwellian, unaffected by the collisions. The calculation is a simplified version of the one

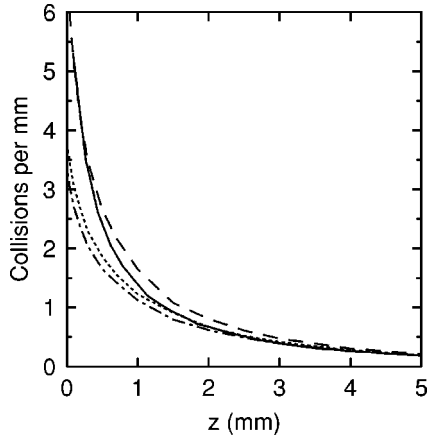

FIG. 2. The number of collisions an average particle experiences per mm as a function of z, the distance from the film, for $Q_0=2.9$ nJ into an 8×8 mm^2 heater. The pulse length is 30 μs for the dashed curve, and 60 μs for the dotted curve. The dash–dot curve is for the Lennard–Jones potential for 60 μs. These calculations do not include the effect of prior collisions on the collision probability at a given z. The full curve, calculated by extrapolation from two simulations for 30 μs, includes the effect of prior collisions, reducing the collision probability for large z.

in Appendix A of Ref. [12]; the main difference is that we simply count collisions rather than checking to see if the scattered atoms hit a target.

The calculation gives $p(z)dz$, the probability that a particle undergoes a collision between z and $z+dz$. The total number of collisions ν_c experienced by an average evaporated atom is

$$\nu_c=\int_0^\infty p(z)dz. \tag{3.1}$$

From the dashed and dotted curves in Fig. 2, $\nu_c=6.6$ for $2\tau=30$ and 5.2 for 60 μs. In the analytical approximation, $p(z)$ and ν_c are simply proportional to Q, which is the same as Q_0. Even for the smallest Q we have considered, 1.4 nJ, the average atom collides with more than two others. The figure also contains a dot–dash curve calculated for $2\tau=60$ μs from the Lennard–Jones potential. At small z, this is about 10% below the dotted curve for the SAPT2 potential.

Figure 2 shows that most of the scattering takes place near the surface of the film, within a characteristic distance $\bar{v}\tau$. Here $\bar{v}$ is the mean speed in the Maxwellian distribution. For the curves in Fig. 2, $\bar{v}\tau=0.8$ and 1.6 mm for $2\tau=30$ and 60 μs. There is also a longer range tail in $p(z)$ on the scale of the heater size. When most of the scattering is close to the surface, the quantity that determines $p(z)$ is the heat input per unit area Q/A rather than Q.

The full curve in Fig. 2 is for $2\tau=30$ μs calculated from the simulation. It therefore has the correct distribution at all z. We extrapolated to $\lambda=1$ from simulations with $r_c(0)=1$ and 2 mm. The simulations used the same Q_0 as the analytical approximation. As expected, $p(0)$ is the same (within the error) in the two methods. The ν_c from the simulation is 5.7 compared to 6.6 from the analytical approximation.

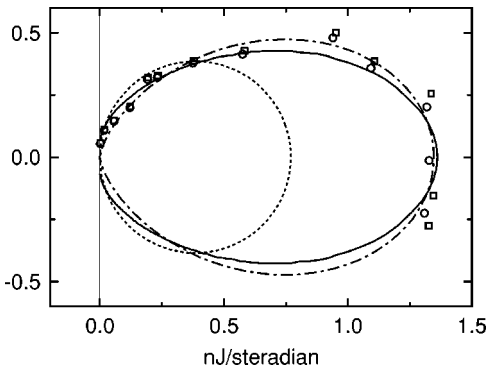

FIG. 3. Polar plot of the energy received on the bolometer in Ref. [1] (circles) and the extrapolation of our simulation (full curve). The experiment in Ref. [1] had the heater offset slightly; the squares are the circles corrected to account for the offset. The dot–dash curve is $\cos^{5/2}\theta$ fitted to the experimental data. The dotted circle is Lambert's law ($\cos\theta$) with the same energy (summed over all directions) as the $\cos^{5/2}\theta$ curve.

B. Dome configuration

In their angular distribution experiment, Eckardt *et al.* [1] used a 4.3 nJ pulse in an 8×8 mm^2 heater coated with a superfluid ^{4}He film. The pulse length was not clearly specified; it was between 10 and 40 μs. They measured the energy received by an identically sized bolometer moved along an arc of radius 35 mm centered on the heater. As shown by the data points in Fig. 3, the angular dependence of the signal did not obey Lambert's law. The intensity in the forward direction is greater, resembling a $\cos^{5/2}\theta$ distribution.

We simulated the experiment of Eckardt *et al.* using $Q=2.7$ nJ and a pulse length of 30 μs. The size of Q was chosen to agree with our estimate of the total heat carried away by the evaporated atoms in the experiment [23]. We used our first configuration which reproduces the bolometer distance in the experiment. The results of the simulation were scaled to the solid angle subtended by the bolometer. This allowed us to improve the statistics compared to just counting the particles hitting the bolometer.

Figure 4 shows some results from this simulation. To find when the scaling method breaks down, we have displayed the total energy per zone, integrated over time, for $r_c(0)=2$, 5, and 10 mm divided by that for $r_c(0)=1$ mm. The deviations from unity are roughly linear in $r_c(0)$, so it is possible to extrapolate to the very small value of $r_c(0)$ that corresponds to the physical result, $\lambda=1$.

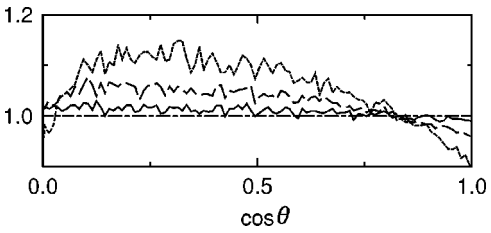

FIG. 4. Comparison of the simulated angular distribution for various values of $r_c(0)$. The graph shows the total energy (kinetic plus binding energy) per unit solid angle for $r_c(0)=2$ mm (full curve), 5 mm (dashed), and 10 mm (dotted) divided by the result for 1 mm.

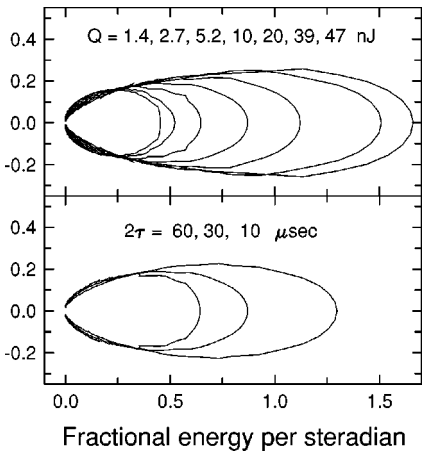

FIG. 5. Polar plot of the fractional energy per steradian for various heat pulses Q and pulse lengths 2τ. The curves show the fraction of the total emitted energy as a function of direction. The upper graph displays results for $2\tau=30$ μs and the heat pulses Q shown. The lower graph is for $Q=10$ nJ.

The figure shows that the difference between $r_c(0)=1$ and 2 mm is approximately 1%. This means that the error in using just the results for $r_c(0)=2$ mm, without extrapolation, is only 2%. To calculate the 2 mm results ($nS=12\times10^6$) took approximately 3.5 days on a 400 MHz Pentium II. The 1 mm data took two weeks.

The full curve in Fig. 3 is an extrapolation of our simulation to $\lambda=1$. The agreement between the data points and the full curve shows that the angular distribution can be explained by evaporation of the film according to Lambert's law followed by scattering just above the film. Obviously, in the limit of $Q=0$, the final distribution must tend to $\cos\theta$ since there will be too few atoms to scatter. Unfortunately, there are no direct measurements of the angular distribution at other intensities to determine its dependence on Q.

We repeated the simulation for other heat pulses and found that the distribution depends strongly on Q and τ, as shown in Fig. 5. These results were extrapolated from $r_c(0)=2$ and 4 mm for large Q and 1 and 2 mm for small Q. As expected, the distribution becomes more collimated in the forward direction as Q is increased or τ is decreased. Note that the figure shows the fraction of the evaporated energy per unit solid angle $f(\theta)$, including the latent heat, so that each of the curves has

$$2\pi\int_0^1 f(\theta)\,d\cos(\theta)=1. \tag{3.2}$$

In addition to the collimation seen in Fig. 5, the average kinetic energy E_k of atoms in the forward direction is increased at the expense of those at large θ. Figure 6 displays E_k divided by the average emitted value $2k_BT$ as a function of angle for various Q. For the largest $Q=39$ nJ, the E_k for $\theta=0$ is more than three times as large as that for $\theta\simeq90°$.

The speed distributions for two different Q and for $\langle\cos\theta\rangle=0.95$ and $\langle\cos\theta\rangle=0.05$ are shown in Fig. 7 as the full curves. Normalized to unity, they are compared to Maxwellian beam distributions with the same average kinetic energy, shown as the dashed curves. Particularly for the larger Q, the distribution for $\langle\cos\theta\rangle=0.95$ is narrower than the

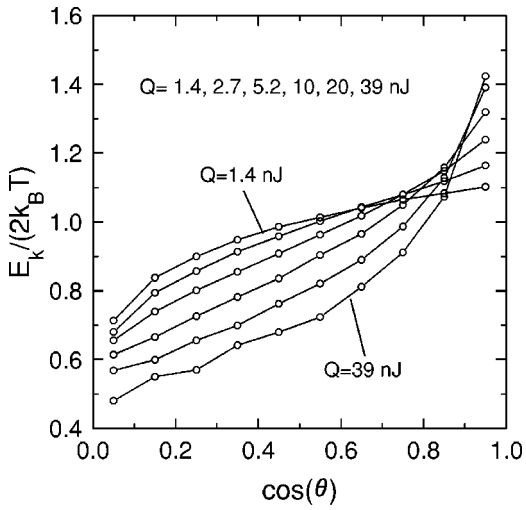

FIG. 6. Mean kinetic energy per atom E_k, divided by the mean evaporated energy $2k_BT$, vs $\langle\cos\theta\rangle$ for various heat pulses Q. The circles are the results of the simulation. In order of increasing steepness, the results correspond to $Q=1.4$, 2.7, 5.2, 10, 20, and 39 nJ.

Maxwellian, i.e., cooler in the center of mass frame. In contrast, the curves at large θ are broader than the Maxwellian. Our simulations are limited by the computation time to Q smaller than ~50 nJ, otherwise it would have been interesting to simulate situations with larger intensities where beam cooling is more pronounced [9].

The theory of beam cooling has been developed in semianalytic form by Toennies and Winkelmann [10]. However their theory is for a steady state with spherical symmetry and so it is not directly applicable to our situation. We postpone a comparison between experiment and our simulated speed distributions to Sec. III D.

The qualitative explanation of the angular effects we observe may be the following: Atoms traveling in the forward direction are less likely to scatter because they quickly move

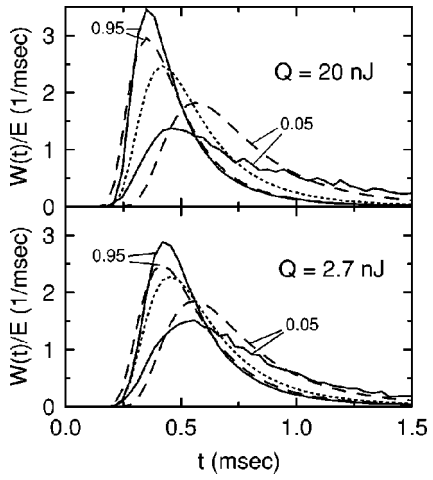

FIG. 7. Fractional speed distributions $W(t)/E$ at a bolometer 35 mm away from the heater. The angles correspond to $\langle\cos\theta\rangle=0.05$ and 0.95; the pulse width is $2\tau=30$ μs. The full curves are the simulation, the dashed curves are Maxwellian beam distributions with temperatures calculated from the average kinetic energy E_k in the corresponding simulation (see Fig. 6). The dotted curves are the original Maxwellian distribution with temperature T.

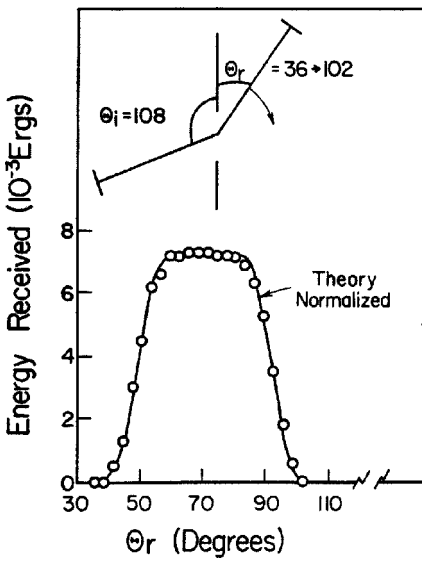

FIG. 8. The window experiment from Ref. [1] (part of Fig. 3 in that paper). A heater and a bolometer are mounted on rotating arms, as shown at the top of the figure. On the left the heater is held at a fixed angle while the bolometer on the right is rotated between measurements with $Q=68$ nJ. The signal on the bolometer as a function of its position (angle of the arm) is shown on the graph as the circles. The full curve is a calculation assuming no scattering, scaled to agree with the intensity in the center of the plateau.

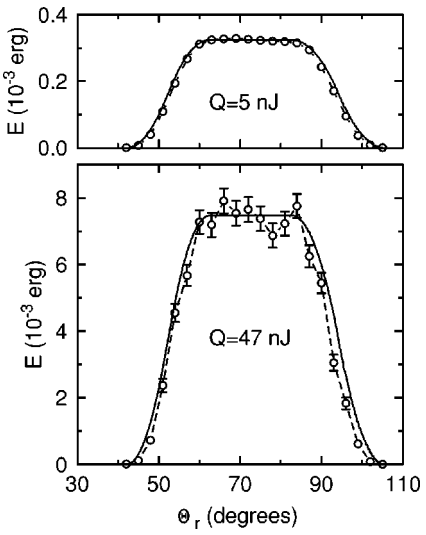

FIG. 9. Simulation of the window experiment shown in Fig. 8. The circles joined by dashed lines show our simulations with $2\tau=30$ μs and $Q=47$ nJ (bottom panel) and $Q=5$ nJ (top). The full curves are the ballistic calculation scaled to match the energy at the plateau.

away from the heater. Atoms traveling at a large angle θ pass by a larger number of other atoms, increasing their chance of scattering. If they are scattered into the forward direction, the probability of another collision decreases. In addition, the effect of such a collision is smaller because v_r is smaller. Thus we have a larger number of atoms with small θ compared to the original distribution.

The enhancement of the energy per particle might be explained by noting that the slower atoms pass by fewer other atoms before the heat pulse ends. Thus it is the fast, large θ atoms that get scattered into the forward direction.

C. Window configuration

Eckardt *et al.* [1] measured the angular distribution of a beam that passed through a window, as shown in Fig. 8. At the top of the figure is a schematic of the experiment. On the left-hand side is a heater on an arm 41 mm long whose axis of rotation passes through the center of the window. A bolometer is mounted on an identical arm on the right. The heater was held in a fixed position while the bolometer arm was rotated between measurements. A signal is detected only over a small range of bolometer angles. This is the width of the beam passing through the window.

Eckardt *et al.* compared their results, produced by a heat pulse of 68 nJ, to a ballistic calculation with no interatomic collisions. This is shown as the full curve in Fig. 8, scaled to fit the height of the signal; it agrees well with the experiment.

We simulated the window experiment using a Q of 47 nJ and $2\tau=30$ μs and found results similar to those in the experiment but with an interesting difference. Our results, shown in Fig. 9, were extrapolated from simulations with $r_c(0)=2$ and 4 mm. At 47 nJ, the difference between the 2 mm results and the extrapolation is quite large, about 10%, because of the strong collimation at this large heat input. Figure 9 shows the surprising result that scattering narrows the beam slightly. We repeated the simulation without scattering to confirm that there was no inconsistency between the simulation and the ballistic calculation. They agreed perfectly.

Although the heat input in the experiment is larger than in the simulation (68 compared to 47 nJ), this could easily be due to losses via heat conduction, etc. Therefore, we consider the agreement between the absolute intensities in Fig. 8 and in the graph at the bottom of Fig. 9 to be useful, if indirect, evidence for the strong collimation predicted by the simulation. From Fig. 5, for $Q=47$ nJ, this is an enhancement of $\sim 2\pi\times 1.56\simeq 10$ compared to Lambert's law.

It is interesting to compare the narrowing with results from our simulation [12] of the proposed cross-section experiment. There we observed only a very small tail on each side of the beam when compared with no scattering. However, only collisions beyond the first set of slits (at 40 mm) were included. This indicates that the narrowing is due to collisions near the heater, as expected. The small tails can still be found in the present simulation. They are too tiny to be seen in Fig. 9.

Calculation of results like those in Fig. 9 is quite tedious so we have not been able to study the dependence on Q and τ in detail. Results with $Q=5$ nJ, shown in the top panel in Fig. 9, and 10 nJ, which has the same degree of narrowing as 47 nJ, indicate that the narrowing is independent of Q if each atom collides with at least 30 or 40 other atoms. For 2.7 nJ, when the number of collisions per atom is 5.7, the narrowing is barely visible. At 5 nJ, shown at the top of Fig. 9, the number of collisions per atom is about 20.

Our tentative explanation for the narrowing is based on an optical analogy. The scattering near the film tends to turn the mean velocity of the atoms towards the forward direction, roughly in proportion to θ. This acts like a converging lens.

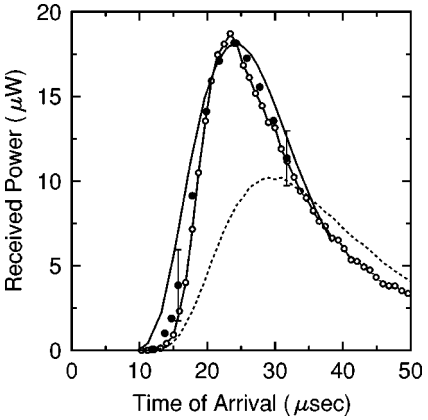

FIG. 10. Power received by the bolometer as a function of time-of-flight in the experiment by Andres *et al.*, Ref. [2]. The full circles are the data in arbitrary units, with two representative error bars. The full curve was fitted by Andres *et al.* to their data. It corresponds to a Maxwellian distribution with temperature 1.1 K. The open small circles are the simulation from an initial Maxwellian with $T=0.756$ K. The dotted curve is the simulation with no scattering.

As seen from the slit, the atoms appear to come from a film further away from the detector. In agreement with this idea, a ballistic calculation with the heater moved 3 mm further away gives very good agreement with the results for 47 nJ in Fig. 9. We have not been able to make a quantitative model to explain why this distance is 3 mm. However, for 5 and 20 nJ, we did try the effect of halving the heater dimensions. This reduced the narrowing, consistent with moving the ''image'' of the heater back half as far.

D. Speed distribution

We now turn to the results for the speed distribution. In Fig. 10 we compare a simulation to the experimental results of Andres *et al.* [2]. The geometry is a 3.7×3.7 mm^2 heater at a distance of 2.34 mm from a similarly sized bolometer. The experimental heat pulse was 1.8 nJ in $2\tau=0.5$ μs; the signal power was measured in arbitrary units. The full curve in the figure corresponds to a Maxwellian distribution with temperature 1.1 K. It was fitted by Andres *et al.* to their data. They also measured a much larger heat input, 180 nJ, for which the fitted Maxwellian corresponds to 2.9 K. We are unable to simulate the large heat pulse experiment because the computation time would be too long.

In the simulation in Fig. 10, we extrapolated to $\lambda=1$ from $r_c(0)=0.5$ and 1 mm. The heat Q was adjusted to 0.84 nJ to give the peak signal at roughly the same time as in the experiment. Compared to the calculations in Figs. 2, 5, and 6, the simulated Q/A corresponds to about 4 nJ into an 8×8 mm^2 heater. However, $\overline{v}\tau$ is only 0.016 mm. In the simulation, the emission temperature T is 0.756 K. With no scattering, this gives the dotted curve in the figure. As one can see, the effect of the scattering is to raise the effective temperature (average kinetic energy) by roughly 1.5. According to the simulation, the mean number of collisions per particle ν_c is 10.

Although the arbitrary units in the data give some flexibility in the comparison, the agreement between the simulation and the experiment in Fig. 10 is fairly good. The Maxwellian at 1.1 K does not fit so well; the data and the simulation rise later and more steeply and have a narrower peak. The simulation is slightly narrower and steeper than the data.

We have also compared our simulation with the power versus time-of-flight data from Ref. [1] at $Q=68$ nJ and from Ref. [3] at $Q=48$ nJ. In both experiments, the beam was observed after passing through the window in the screen, so that the range of θ was quite narrow. The value of 2τ is not well-defined in these experiments. A model [20] of the film/heater combination indicates that evaporation takes place in a rounded peak about 30 μs wide. The agreement between these data and our simulation is only semiquantitative; the simulated signal is more energetic (higher average energy per atom) and narrower in distribution (cooler in the center of mass).

These discrepancies might be due to several factors. As we have seen, the results of the simulation are not very sensitive to the potential, and it is difficult to accept that three-body collisions are the problem. The time constant of the bolometer in Ref. [3] was estimated to be ~50 μs. We recalculated the simulation to correct for this but the disagreement remained. The most likely cause for the discrepancies, in our opinion, is the time dependence of the evaporation rate in the experiment. If the film temperature was known as a function of time, it could be included in the simulation, giving a more rigorous test of the theory.

IV. CONCLUSION

Except for some of the speed distribution measurements, the agreement between the simulation and experiment is quite good. The strong effect of atomic scattering near the surface of the film is clearly demonstrated, and it must always be taken into account in interpreting the distribution far away from the film. In our simulation, we have assumed the initial evaporated distribution to be Maxwellian. So far, we have no reason to discard this assumption. It could be tested more rigorously by measuring the temperature of the evaporating film during the heating pulse, and using the results in the simulation.

In some experiments, the evaporated beam has been assumed to propagate ballistically. How does the scattering near the film change the interpretation of such experiments? The only measurements seriously affected are those of the emitted distribution itself [1–3]. The measurements of the reflection of atoms at the surface of the liquid [4–6] or of the atomic cross section [7,8,12], are not significantly influenced by scattering near the film. In those experiments, the spatial and speed distribution of the incident beam was observed independently and properly taken into account in the measurement. This is also true for the proposed experiment on the low energy cross section that we simulated in Ref. [12]. Some of the effects due to intrabeam scattering can be beneficial in making the speed distribution more homogeneous at large Q or in collimating the beam in the forward direction.

ACKNOWLEDGMENTS

This work was supported by NSF Grant No. DMR 9630930. We are grateful to Dr. S. Mukherjee for valuable discussions and assistance.

[1] J. Eckardt, D.O. Edwards, F.M. Gasparini, and S.Y. Shen, in *Proceedings of the 13th International Conference on Low Temperature Physics LT-13*, edited by K. D. Timmerhaus, W. J. O'Sullivan, and E. F. Hammel (Plenum, New York, 1974), p. 518.
[2] K. Andres, R.C. Dynes, and V. Narayanamurti, Phys. Rev. A **8**, 2501 (1973).
[3] D.O. Edwards, G.G. Ihas, and C.P. Tam, Phys. Rev. B **16**, 3122 (1977).
[4] D.O. Edwards *et al.*, Phys. Rev. Lett. **34**, 1153 (1975).
[5] V.U. Nayak, D.O. Edwards, and N. Masuhara, Phys. Rev. Lett. **50**, 990 (1983).
[6] A.F.G. Wyatt, M.A.H. Tucker, and R.F. Cregan, Phys. Rev. Lett. **74**, 5236 (1995).
[7] J.C. Mester *et al.*, J. Low Temp. Phys. **89**, 569 (1992).
[8] J.C. Mester *et al.*, Phys. Rev. Lett. **71**, 1343 (1993).
[9] E.S. Meyer, J.C. Mester, and I.F. Silvera, Phys. Rev. Lett. **70**, 908 (1993).
[10] J.P. Toennies and K. Winkelmann, J. Chem. Phys. **66**, 3965 (1977).
[11] E.S. Meyer, Ph.D. thesis, Harvard University, 1993.
[12] H.H. Hjort, S.A. Viznyuk, and D.O. Edwards, J. Low Temp. Phys. **116**, 99 (1999).
[13] F. Luo, G.C. McBane, G. Kim, and C.F. Giese, J. Chem. Phys. **98**, 3564 (1993).
[14] A.R. Janzen and R.A. Aziz, J. Chem. Phys. **107**, 914 (1997).
[15] E. Meiburg, Phys. Fluids **29**, 3107 (1986).
[16] H.A. Bethe, Phys. Rev. **76**, 38 (1949).
[17] Y.H. Uang and W.C. Stwalley, J. Phys. (Paris) **41**, C7–33 (1980).
[18] T. Korona *et al.*, J. Chem. Phys. **106**, 5109 (1997).
[19] The simulation and other associated programs have been posted at the web page http://www.physics.ohio-state.edu/~hjort/programs.
[20] P.M. Mrozinski, Ph.D. thesis, The Ohio State University, 1974.
[21] R. de Bruyn Ouboter and C.N. Yang, Physica B **144**, 127 (1987).
[22] R.L. Rusby, J. Low Temp. Phys. **58**, 203 (1985).
[23] The angular distribution data in Ref. [1] have been increased by a factor of 10. We believe the energy scale in their Fig. 2 should be in 10^{-5} erg rather than 10^{-6} erg. This is based on an estimate of the total energy of the evaporated atoms in their experiment. From an approximate integral of their angular distribution without our correction, the evaporated energy is only 0.27 nJ compared to their total heat input 4.3 nJ. Applying our factor of 10, we have compared their data with a simulation with $Q=2.7$ nJ.